ChemComm

COMMUNICATION

View Article Online
View Journal | View Issue

Cite this: *Chem. Commun.*, 2014, **50**, 7176

Received 19th March 2014,
Accepted 16th May 2014

DOI: 10.1039/c4cc02037e

www.rsc.org/chemcomm

Control of emission colour with N-heterocyclic carbene (NHC) ligands in phosphorescent three-coordinate Cu(I) complexes†

Valentina A. Krylova, Peter I. Djurovich, Brian L. Conley, Ralf Haiges, Matthew T. Whited, Travis J. Williams and Mark E. Thompson*

A series of three phosphorescent mononuclear (NHC)–Cu(I) complexes were prepared and characterized. Photophysical properties were found to be largely controlled by the NHC ligand chromophore. Variation of the NHC ligand leads to emission colour tuning over 200 nm range from blue to red, and emission efficiencies of 0.16–0.80 in the solid state.

Phosphorescent Cu(I) complexes are an emerging class of luminescent materials based on an inexpensive and abundant metal.[1] The ability to tune chemical and photophysical properties in a desirable and predictable way is highly important when considering potential applications of Cu(I)-based phosphors. The typical strategy to modulate the excited state properties of these and related luminescent materials is usually achieved through variation of the coordinating ligand(s).[2] To date the types of ligands most commonly used to prepare phosphorescent Cu(I) complexes are diimines or organophosphines and their derivatives.[3] Alternatively, N-heterocyclic carbenes (NHC) are an attractive class of ligands as they are electronically and sterically tunable and form strong bonds with transition metals giving robust complexes.[4] However, while NHCs have been employed as either chromophoric or ancillary ligands in luminescent Ir and Pt complexes[5] they have been rarely used as chromophoric ligands in Cu(I) complexes.[6]

We have recently used NHC ligands to prepare phosphorescent 3-coordinate Cu(I) complexes (NHC)Cu(N^N), where N^N denotes a neutral diimine or monoanionic pyridyl-azolate ligand.[7] The monodentate NHC ligand, 1,3-bis(2,6-diisopropylphenyl)imidazol-2-ylidene (IPr), employed in these complexes has both a large π–π^* energy gap and high triplet energy, therefore the emission energy in these derivatives is controlled by variations in the N^N ligand.

Department of Chemistry, University of Southern California, Los Angeles 90089-0744, USA. E-mail: met@usc.edu

† Electronic supplementary information (ESI) available: Experimental and computational details, synthesis and characterization of new compounds, absorption data for precursors and (IPr)Cu(pz_2BH_2) complex, photophysical data for **1–3** obtained at 77 K in the solid state and in methylcyclohexane glass and crystallographic data. CCDC 976577–976579 and 990891. For ESI and crystallographic data in CIF or other electronic format see DOI: 10.1039/c4cc02037e

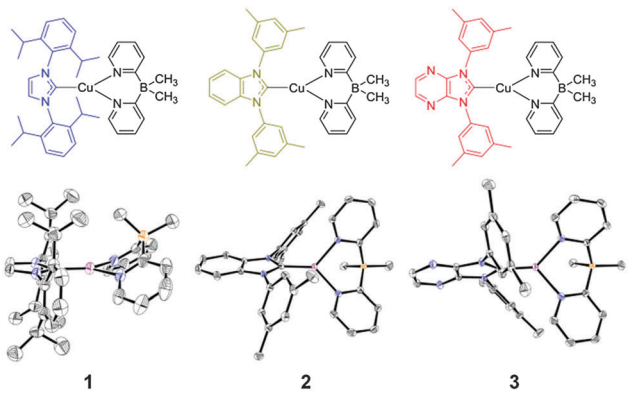

Fig. 1 Molecular structures (top) and perspective view at 50% probability (bottom) of complexes **1–3**. Only one of the unique structures for **2** found in the unit cell is shown. Hydrogen atoms are omitted for clarity.

Herein, we report a series of luminescent (NHC)Cu(N^N) complexes **1–3** (Fig. 1), where the NHC ligand is principally involved in the excited state and demonstrate a wide range emission colour tunability through modification of carbene moiety. In particular, we systematically lowered the energy gap of **1** by benzannulation of imidazolylidene ring to make **2** and further introduced nitrogen atoms to form the pyrazinyl moiety in **3**. In addition, we utilize an anionic non-conjugated N^N ligand, *i.e.* di(2-pyridyl)dimethylborate (py_2BMe_2) that possesses high triplet energy to serve as an ancillary ligand.[8] To the best of our knowledge the py_2BMe_2 ligand, unlike the isoelectronic di(1-pyrazolyl)borates (pz_2BR_2, R = H, alkyl, aryl),[2c,9] has never been used to prepare luminescent transition metal complexes. We have found that (NHC)Cu complexes with the py_2BMe_2 ligand are more robust and luminescent than the pyrazolyl-borate congeners.

The (NHC)Cu(py_2BMe_2) complexes were obtained from their respective (NHC)CuCl precursors upon addition of a stoichiometric amount of sodium di(2-pyridyl)dimethylborate in tetrahydrofuran at RT. Complexes **1–3** are stable in solid state and in solution under anaerobic conditions. Complex **1** can be sublimed under vacuum and is stable for hours in solution, while **2** and **3** decompose slowly under aerobic conditions in solution and blacken in the solid state

after 24 h exposure to air. Evidently, the isopropyl groups at *ortho* positions of phenyl groups of the NHC ligand in **1** impart greater stability of the (NHC)Cu(py_2BMe_2) complexes than in **2** and **3**. We also prepared complexes analogous to **1** and **2** using the pz_2BH_2 ligand instead of py_2BMe_2. While the analog to **1**, (IPr)Cu(pz_2BH_2), can be isolated and fully characterized (see ESI†), the congener to **2** decomposed rapidly upon exposure to air and was not examined further.

X-ray diffraction analyses confirmed monomeric three-coordinate structures for complexes **1–3**. Complex **2** has two unique structures in the unit cell that have similar geometric parameters. The coordination geometry in complexes **1–3** can be described as Y-shaped with the sum of bond angles around copper close to 360° (359.98° in **1**, 359.72° in **2** and 358.64° in **3**). The Cu–N–C–B–C–N ring formed upon chelation of the py_2BMe_2 ligand adopts a boat-shaped conformation similar to that reported in metal complexes bearing related di(2-pyridyl)borate ligands.[8,10] The relative orientations of NHC and py_2BMe_2 ligands in crystals differ within the series. In complex **1** the ligands are arranged with the pyridyl rings situated opposite the aryl rings of the NHC ligand across a crystallographic mirror plane that bisects the C_{NHC}, Cu and B atoms. In contrast, the py_2BMe_2 ligand in **2** and **3** is oriented about C_{NHC}–Cu bond so that the two pyridyl rings are situated above and below a plane defined by the N_{NHC}, N_{NHC} and C_{NHC} atoms. The Cu–N_{py} bond lengths in **1** are 2.0288(15) Å and slightly shorter in **2** (1.9929(16) Å and 1.9997(16) Å) and **3** (2.010(9) Å and 2.014(9) Å). The C_{NHC}–Cu–N_{py} angles are 132.78(4)° in **1** and vary from 134.32(7)° and 129.27(7)° in **2** to (135.0(6)° and 128.1(6)°) in **3**. The C_{NHC}–Cu distances in **1–3** (1.8678(19)–1.895(2) Å) are within the range for reported NHC–Cu(I) complexes.[11]

In solution ^{1}H NMR data indicates rapid boat-to-boat interconversion of the py_2BMe_2 ligand as resonances of methyl groups attached to boron atom appear as one broad singlet both at room temperature and at −40 °C in acetone-d_6. Although the ^{1}H NMR data do not allow us to assess if there is free rotation about the C_{NHC}–Cu bonds in solution, the chemical shift for the protons *ortho* to the pyridyl nitrogens gives insight into the preferred molecular conformation. This resonance appears at δ = 8.36 ppm in the protonated $py_2BMe_2^-$ ligand, whereas upon coordination to copper in **1** it is shifted markedly upfield to δ = 7.3 ppm due to shielding by the diamagnetic ring current from the adjacent aryl rings of the NHC ligand. In contrast, the same resonance undergoes a much smaller shift upon coordination in **2** and **3**, appearing at δ = 7.97 ppm and δ = 8.05 ppm, respectively. Thus, the ^{1}H NMR data in solution correlate with the relative ligand orientation found in crystalline state; co-planar for **1**, perpendicular for **2** and **3**.

Photophysical data for complexes **1–3** are summarized in Table 1. The UV-visible absorption spectra for complexes **1–3** in dichloromethane are shown in Fig. 2. High energy bands at 290 nm in **1** ($\varepsilon \sim$ 7000–14 200 M^{-1} cm^{-1}), 310 nm in **2** ($\varepsilon \sim$ 6500–19 000 M^{-1} cm^{-1}) and 340 nm in **3** ($\varepsilon \sim$ 4000–13 400 M^{-1} cm^{-1}) are assigned to spin-allowed ligand centered (LC) transitions on both the NHC and py_2BMe_2 ligands. Lower energy bands, not observed in absorption spectra of precursors (see ESI†), are assigned to charge transfer (CT) transitions. In complex **1** the CT bands appear at 316 nm (ε = 6100 M^{-1} cm^{-1}) with a shoulder at 360 nm ($\varepsilon \sim$ 1300 M^{-1} cm^{-1}). A comparison between the absorption spectrum of **1** to that of (IPr)Cu(pz_2BH_2) (see ESI†) shows the LC band is unchanged in energy in both derivatives, whereas the CT bands shift to higher energy and lower intensity (λ_{max} = 305 nm, ε = 2000 M^{-1} cm^{-1} and λ_{max} = 330 nm, $\varepsilon \sim$ 1000 M^{-1} cm^{-1}) in the latter complex. The bathochromic shift for the low energy bands in **1** indicates that the py_2BMe_2 ligand participates in these transitions, although some CT character involving the IPr ligand may contribute as well. Upon expansion of π-system of the NHC ligand in **2** the CT band becomes more distinct and intense (λ_{max} = 346 nm, ε = 9100 M^{-1} cm^{-1}). Substitution of the two CH-groups with nitrogens in **3** leads to a marked red shift and increase in molar absorptivity (λ_{max} = 422 nm, ε = 10 300 M^{-1} cm^{-1}). Thus, these bands in **2** and **3** are unambiguously assigned to CT transitions involving NHC ligands.

The emission spectra recorded for neat microcrystalline solids of complexes **1–3** at room temperature are broad and featureless (Fig. 2). Complex **1** gives sky-blue emission (λ_{max} = 476 nm), complex **2** displays yellow emission (λ_{max} = 570 nm) and **3** has orange-red emission (λ_{max} = 638 nm). The bathochromic shift in emission for complexes **2** and **3** further indicates that the lowest energy excited state is governed largely by the NHC ligand. Solid powders of **1** and **2** glow brightly upon excitation with emission quantum yields (Φ) of 0.80 and 0.70 respectively, while **3** has moderate emission efficiency (Φ = 0.16). In contrast, the quantum efficiency of the (IPr)Cu(pz_2BH_2) derivative in the solid state is much lower (λ = 415 nm, Φ = 0.03). The observed luminescence for **1–3** is phosphorescence as emission lifetimes (τ) are in the microsecond regime. The radiative rate constants (k_r) in the solid state vary within the small range of values (k_r = (3.3–7.2) × 10^4 s^{-1}). In fluid solution the emission efficiency is substantially lower than in the solid state. In particular, complex **1** has quantum yield of 0.15 (τ = 2.3 μs) in cyclohexane, while emission from **2** and **3** is almost completely quenched (Φ < 0.005).

The emission spectra of neat samples of **1–3** shift to lower energies upon cooling to 77 K (Table 1, also see ESI†). Bathochromic shifts in emission energy at low temperature are common for Cu(I) complexes. This phenomenon is often attributed to suppression of thermally activated delayed fluorescence (TADF) and usually accompanied by a marked increase in emission

Table 1 Photophysical data for complexes **1–3**

		Emission at room temperature[b]					Emission at 77 K[b]	
	Absorbance,[a] λ (nm) ε (10^3 M^{-1} cm^{-1})	λ_{max} (nm)	τ (μs)	Φ	k_r (s^{-1})	k_{nr} (s^{-1})	λ_{max} (nm)	τ (μs)
1	268 (14.2), 316 (6.1), 360 sh (1.3)	476	11	0.8	7.2 × 10^4	1.8 × 10^4	492	36
2	257 sh (19.3), 346 (9.1)	570	15	0.7	4.7 × 10^4	2.0 × 10^4	586	17
3	271 (13.3), 305 (7.4), 422 (10.3)	638	7.5	0.16	3.3 × 10^4	1.0 × 10^5	650	21

[a] In dichloromethane. [b] In solid state.

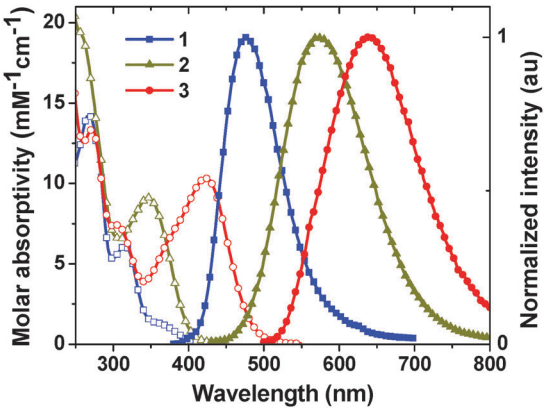

Fig. 2 Absorption (open symbols, CH_2Cl_2) and emission (closed symbols, solid powder) spectra of complexes **1–3** at room temperature.

lifetimes of an order of magnitude or more.[9,12] Complexes **1–3**, however, show only a modest increase in emission lifetimes upon cooling as emission lifetimes measured at 77 K are in the range of 17–36 μs (Table 1). The relatively small increase in lifetime at 77 K is inconsistent with processes typically associated with TADF and suggests instead that emission measured both at room temperature and 77 K is from a state that is principally triplet in character. The behavior also implies that the radiative rate constant for the lowest triplet state is significantly enhanced in **1–3**. This unusual temperature dependence on the emission lifetime is being currently investigated in greater detail at lower temperatures.

The observed bathochromic shift of emission energy in **1–3** upon expanding the size of the π-system of a ligand chromophore and N-substitution is consistent with a decrease in separation between the highest occupied molecular orbital (HOMO) and the lowest unoccupied molecular orbital (LUMO). Computational analyses of the ground and excited state properties performed using density functional theory (DFT) and time-dependent DFT (TD-DFT) calculations compare favorably with the experimental observations. The calculated wavelength and oscillator strength of the lowest singlet transitions progressively increase for **1** (λ = 381 nm, f = 0.0028), **2** (λ = 400 nm, f = 0.1440) and **3** (λ = 522 nm, f = 0.1645). This result follows the trend observed in absorption spectra, *i.e.* a decrease in energy and increase of molar absorption for the CT bands when going from **1** to **2** to **3**. The frontier molecular orbitals for **1–3** are shown in Fig. 3A. For all three complexes the calculated HOMOs have essentially identical spatial contours, consisting predominantly of d orbitals on copper (39–48%) mixed with orbitals on di(2-pyridyl)dimethylborate ligand (41–45%). The LUMO in **1–3** is localized on the NHC ligand (85–94%) with minimal metal character (4–6%). A small contribution (8%) from the py_2BMe_2 orbitals appears in the LUMO of complex **1**; however, there is less (4% and 2%) in both **2** and **3**. Noteworthy is a substantial contribution (8–23%) from the carbene carbon $2p_z$ orbital in the LUMO of all three complexes. Congruent with the orbital composition, variations of the carbene ligand have pronounced effect on LUMO energies. Complex **1** has the highest LUMO energy in the series (E_{LUMO} = −0.58 eV) followed

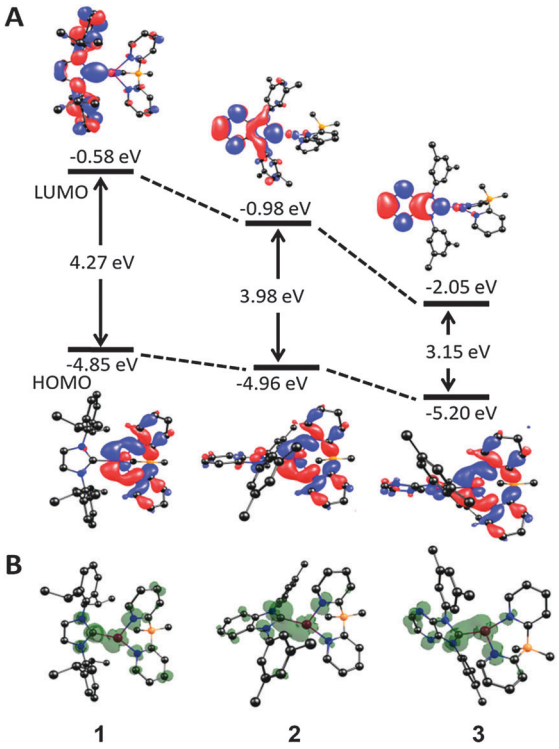

Fig. 3 (A) HOMO and LUMO plots and energies for **1–3**. (B) Optimized triplet geometries and triplet spin density contour plots (isovalue: 0.004 e a_0^{-3}). Hydrogen atoms are omitted for clarity.

by **2** (E_{LUMO} = −0.98 eV) and **3** (E_{LUMO} = −2.05 eV). The HOMO energies show a similar trend in stabilization, albeit to a lesser degree (E_{HOMO} = −4.85 eV, −4.96 eV, −5.20 eV, for **1–3**, respectively). The HOMO–LUMO gap is thus progressively smaller for **1** (ΔE_{H-L} = 4.27 eV), **2** (ΔE_{H-L} = 3.98 eV) and **3** (ΔE_{H-L} = 3.15 eV).

The lowest vertical singlet and triplet excitations obtained from TD-DFT calculations are mainly HOMO → LUMO transitions (see ESI†). On the basis of the MO description given above the lowest lying transition for complex **1** can be ascribed as (M + L)LCT admixed with intraligand π → π* (py_2BMe_2) (ILCT) character, whereas for complexes **2** and **3** the transition is principally metal–ligand to NHC–ligand charge transfer ((M + L)LCT). The calculated spin density surfaces for the triplet electronic configuration further support this assignment (Fig. 3B). For complexes **1–3** the spin contours are localized along the C_{NHC}–Cu bond axis. Both ligands also contribute to the triplet spin density; however, while complex **1** has a significant contribution from the borate ligand (31% NHC, 31% py_2BMe_2), the spin distribution is shifted toward NHC ligand for complexes **2** (52% NHC, 16% py_2BMe_2) and **3** (54% NHC, 16% py_2BMe_2).

To emphasize the importance of proper ligand design to achieve efficient room temperature phosphorescence from this family of Cu(I) compounds, we prepared complex **4** where the π-system of the NHC ligand was expanded by annulation of imidazolylidene with a peri-naphthyl moiety (Fig. 4, full characterization is given in ESI†). For this derivative, the intensity of the lowest lying CT absorption band centered at 450 nm is low

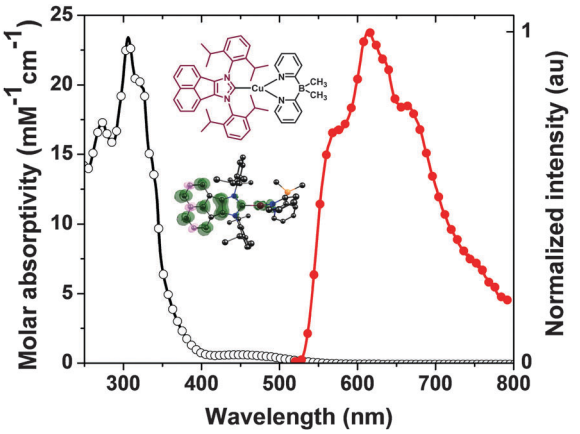

Fig. 4 Absorption (room temperature, CH_2Cl_2) and emission (77 K, 2-MeTHF) spectra of complex **4**. (inset) Molecular structure, optimized triplet geometry and spin density contour plot (isovalue: 0.004 e a_0^{-3}).

(ε = 450 M^{-1} cm^{-1}) and the complex is nonemissive in the solid state at room temperature and at 77 K. Very weak, structured emission (Φ < 0.01, τ < 10 ns) is observed from a dilute solution of **4** in frozen 2-methyltetrahydrofuran (2-MeTHF) glass at 77 K (Fig. 4). This emission is tentatively assigned as phosphorescence since the radiative rate constant ($k_r < 10^6$ s^{-1}) and presence of vibronic features are inconsistent with fluorescence from the CT state. The HOMO for **4** calculated using DFT is essentially identical to that of complexes **1–3**. The LUMO, localized primarily on the aromatic π-system of NHC ligand, has no electron density on the $2p_z$ orbital of C_{NHC} atom in strong contrast to what is found in complexes **1–3**. Such an electronic distribution leads to poor overlap between frontier orbitals and thus a low oscillator strength for the lowest lying CT transitions (λ = 597 nm, f = 0.0044). The triplet spin density of **4** is localized on the acenaphthyl moiety and, unlike that of complexes **1–3**, has a node across the C_{NHC}–Cu bond axis (Fig. 4). The spin distribution, together with structured emission spectrum, suggests that the luminescence is ligand centered in character. Thus, extension of the π-system in this manner, while shrinking the HOMO–LUMO gap (ΔE_{H-L} = 2.55 eV), decreases the energy of the ^{3}LC state on the NHC ligand and reduces electronic coupling to such a degree that it can no longer effectively interact with the MLCT states responsible for promoting fast radiative decay.[3b]

In conclusion, we report a series of (NHC)–Cu(I) complexes that show phosphorescence associated primarily with NHC ligand chromophore. Judicious modification of the NHC ligand allows the emission colour to be tuned over 200 nm from blue to orange-red while retaining high emission efficiencies. The estimated triplet radiative rate constants are comparable with those of third row transition metal complexes. Taking into account electronic and steric tunability of the NHC ligands, these findings introduce a new versatile method to control the photophysical properties of luminescent Cu(I) complexes.

We are grateful to the Universal Display Corporation for financial support. B.L.C. and T.J.W. also thank National Science Foundation CHE-1054910 grant for support. Theoretical calculations were supported by the University of Southern California Center for High-Performance Computing and Communications (www.usc.edu/hpcc). The X-ray diffractometer is sponsored by National Science Foundation CRIF Grant 1048807.

Notes and references

1 A. Barbieri, G. Accorsi and N. Armaroli, *Chem. Commun.*, 2008, 2185.
2 (*a*) J. Brooks, Y. Babayan, S. Lamansky, P. I. Djurovich, I. Tsyba, R. Bau and M. E. Thompson, *Inorg. Chem.*, 2002, **41**, 3055; (*b*) Y. Chi and P.-T. Chou, *Chem. Soc. Rev.*, 2010, **39**, 638; (*c*) J. Li, P. I. Djurovich, B. D. Alleyne, M. Yousufuddin, N. N. Ho, J. C. Thomas, J. C. Peters, R. Bau and M. E. Thompson, *Inorg. Chem.*, 2005, **44**, 1713; (*d*) Y. You and S. Y. Park, *Dalton Trans.*, 2009, 1267.
3 (*a*) G. F. Manbeck, W. W. Brennessel and R. Eisenberg, *Inorg. Chem.*, 2011, **50**, 3431; (*b*) C.-W. Hsu, C.-C. Lin, M.-W. Chung, Y. Chi, G.-H. Lee, P.-T. Chou, C.-H. Chang and P.-Y. Chen, *J. Am. Chem. Soc.*, 2011, **133**, 12085; (*c*) M. Hashimoto, S. Igawa, M. Yashima, I. Kawata, M. Hoshino and M. Osawa, *J. Am. Chem. Soc.*, 2011, **133**, 10348; (*d*) S. B. Harkins and J. C. Peters, *J. Am. Chem. Soc.*, 2005, **127**, 2030; (*e*) D. G. Cuttell, S.-M. Kuang, P. E. Fanwick, D. R. McMillin and R. A. Walton, *J. Am. Chem. Soc.*, 2002, **124**, 6; (*f*) M. G. Crestani, G. F. Manbeck, W. W. Brennessel, T. M. McCormick and R. Eisenberg, *Inorg. Chem.*, 2011, **50**, 7172; (*g*) N. Armaroli, G. Accorsi, F. Cardinali and A. Listorti, *Top. Curr. Chem.*, 2007, **280**, 69; (*h*) S. Igawa, M. Hashimoto, I. Kawata, M. Yashima, M. Hoshino and M. Osawa, *J. Mater. Chem. C*, 2013, **1**, 542–551; (*i*) M. Wallesch, D. Volz, D. M. Zink, U. Schepers, M. Nieger, T. Baumann and S. Braese, *Chem. – Eur. J.*, 2014, **20**, 6578–6590.
4 (*a*) D. Bourissou, O. Guerret, F. P. Gabbaie and G. Bertrand, *Chem. Rev.*, 2000, **100**, 39; (*b*) H. Jacobsen, A. Correa, A. Poater, C. Costabile and L. Cavallo, *Coord. Chem. Rev.*, 2009, **253**, 687.
5 (*a*) Y. Unger, D. Meyer, O. Molt, C. Schildknecht, I. Muenster, G. Wagenblast and T. Strassner, *Angew. Chem., Int. Ed.*, 2010, **49**, 10214; (*b*) K.-Y. Lu, H.-H. Chou, C.-H. Hsieh, Y.-H. O. Yang, H.-R. Tsai, H.-Y. Tsai, L.-C. Hsu, C.-Y. Chen, I. C. Chen and C.-H. Cheng, *Adv. Mater.*, 2011, **23**, 4933; (*c*) T. Sajoto, P. I. Djurovich, A. Tamayo, M. Yousufuddin, R. Bau, M. E. Thompson, R. J. Holmes and S. R. Forrest, *Inorg. Chem.*, 2005, **44**, 7992.
6 (*a*) K. Matsumoto, N. Matsumoto, A. Ishii, T. Tsukuda, M. Hasegawa and T. Tsubomura, *Dalton Trans.*, 2009, 6795; (*b*) R. Visbal and M. C. Gimeno, *Chem. Soc. Rev.*, 2014, **43**, 3551.
7 (*a*) V. A. Krylova, P. I. Djurovich, J. W. Aronson, R. Haiges, M. T. Whited and M. E. Thompson, *Organometallics*, 2012, **31**, 7983; (*b*) V. A. Krylova, P. I. Djurovich, M. T. Whited and M. E. Thompson, *Chem. Commun.*, 2010, **46**, 6696.
8 T. G. Hodgkins and D. R. Powell, *Inorg. Chem.*, 1996, **35**, 2140.
9 R. Czerwieniec, J.-B. Yu and H. Yersin, *Inorg. Chem.*, 2011, **50**, 8293.
10 B. L. Conley and T. J. Williams, *J. Am. Chem. Soc.*, 2010, **132**, 1764.
11 S. Diez-Gonzalez, E. C. Escudero-Adan, J. Benet-Buchholz, E. D. Stevens, A. M. Z. Slawin and S. P. Nolan, *Dalton Trans.*, 2010, **39**, 7595.
12 (*a*) G. Blasse and D. R. McMillin, *Chem. Phys. Lett.*, 1980, **70**, 1; (*b*) J. C. Deaton, S. C. Switalski, D. Y. Kondakov, R. H. Young, T. D. Pawlik, D. J. Giesen, S. B. Harkins, A. J. M. Miller, S. F. Mickenberg and J. C. Peters, *J. Am. Chem. Soc.*, 2010, **132**, 9499; (*c*) M. J. Leitl, F.-R. Kuechle, H. A. Mayer, L. Wesemann and H. Yersin, *J. Phys. Chem. A*, 2013, **117**, 11823.